Mechanical testing of miniature carbon fiber reinforced polymer (CFRP) samples under digital light microscopy

E. S. Statnik
Laboratory of Hierarchically Structured Materials (HSM), Center for Digital Engineering, Skoltech, Russia
CASM&T, MAI, Russia; Laboratory of Accelerated Particles "LUCh", NUST MISIS, Russia
eugene.statnik@skoltech.ru, https://orcid.org/0000-0002-1105-9206

Iu. A. Sadykova
Laboratory of Hierarchically Structured Materials (HSM), Center for Digital Engineering, Skoltech, Russia
iuliia.sadykova@skoletch.ru

E. N. Prokopev
Laboratory of Accelerated Particles "LUCh", NUST MISIS, Russia
syd.ry@mail.ru

A.I. Salimon
Laboratory of Hierarchically Structured Materials (HSM), Center for Digital Engineering, Skoltech, Russia; CASM&T, MAI, Russia; Laboratory of Accelerated Particles "LUCh", NUST MISIS, Russia
a.salimon@skoltech.ru, https://orcid.org/0000-0002-9048-8083

E. V. Nazarov, N. V. Turbin
CASM&T, MAI, Russia
e.nazarov@mai.ru, nikturbin@gmail.com

A.M. Korsunsky
CASM&T, MAI, Russia; Laboratory of Accelerated Particles "LUCh", NUST MISIS, Russia; Laboratory of Hierarchically Structured Materials (HSM), Center for Digital Engineering, Skoltech, Russia
alexander.korsunsky@gmail.com, https://orcid.org/0000-0002-3558-5198

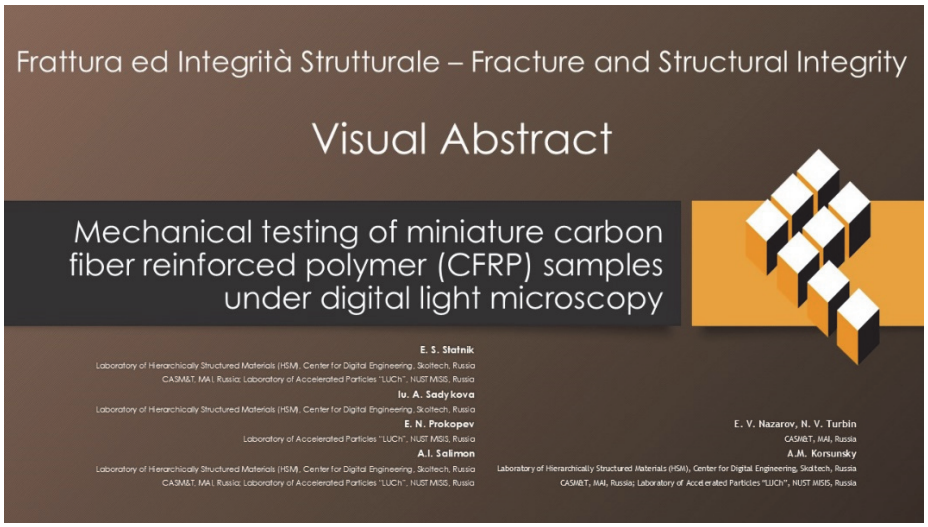

Citation: Statnik, A. N., Sadykova, Iu. A., Prokopev, E. N., Salimon, A.I., Nazarov, E. V., Turbin, N. V., Korsunsky, A.M., Mechanical testing of miniature carbon fiber reinforced polymer (CFRP) samples under digital light microscopy, Fracture and Structural Integrity, 71 (2024) 239-245.

Received: 02.11.2024
Accepted: 19.11.2024
Published: 21.11.2024
Issue: 01.2025

KEYWORDS. Carbon Fiber Reinforced Polymers, Miniature samples, In Situ Mechanical Testing, Digital Light Microscopy, Digital Image Correlation (DIC).

INTRODUCTION

Carbon Fiber Reinforced Polymers (CFRP) are widely valued in modern engineering due to their exceptional strength-to-weight ratio, high durability, and resistance to deformation and fatigue, making them indispensable in industries such as aerospace [1-3], automotive [4,5], and sports [6,7]. These fields demand materials that offer superior performance without compromising weight, and CFRP has emerged as an ideal solution. However, testing CFRP materials presents unique challenges [8,9]. The composite nature of CFRP, which combines fibers and a polymer matrix, introduces heterogeneity and complex load transfer mechanisms. CFRP also exhibits anisotropy, meaning its mechanical properties vary depending on the direction of the load relative to fiber orientation [10-12].

Traditional testing methods, often performed on bulk samples, may not capture the localized behaviors and interactions within CFRP materials, missing crucial details about fiber-matrix interactions and internal stress distributions [9,13,14]. Such limitations create a need for specialized approaches to better understand the mechanical performance of CFRP.

Miniature sample testing addresses these challenges by enabling detailed exploration of local properties, especially important for applications that rely on smaller structural components or require precise characterization of micro-mechanical responses. Testing smaller samples reveals critical behaviors that might otherwise be obscured in larger-scale tests, offering a more accurate understanding of how CFRP materials will perform in real-world applications [13,15-17].

In situ mechanical testing techniques, which allow researchers to observe material deformation and response in real time, are particularly valuable for studying CFRP. Unlike conventional post-test analyses, in situ methods capture dynamic processes as they occur, providing a deeper and more immediate look at deformation, crack initiation, and fiber-matrix interactions [18,19]. This ability to observe mechanical behaviors in real time allows for a more nuanced understanding of how CFRP materials respond to stress, particularly under complex loading conditions.

In light of these advantages, this study aims to investigate the in situ mechanical properties of miniature CFRP samples. By analyzing these aspects at the micro-level, this research seeks to identify failure mechanisms specific to CFRP that contribute to its overall mechanical behavior.

MATERIALS AND METHODS

The CFRP composite plate was fabricated using the resin transfer molding (RTM) technique. In this process, a carbon fiber preform with a lay-up sequence of 0°/90°/0°/90°/0° was placed in a closed mold, and a low-viscosity epoxy resin was injected under pressure to ensure thorough fiber impregnation. The resin pressure was maintained at 5 bar, while vacuum assistance (~0.05 bar) was applied to eliminate any trapped air within the mold prior to injection. The composite was then cured at an elevated temperature of 100°C for 2 hours to achieve optimal cross-linking and mechanical properties.

A dog-bone-shaped specimen, measuring 30×12×0.5 mm, and a rectangular bar with dimensions of 2×4×6 mm were cut from the composite plate using an Accutom-100 cutting machine (Struers, Germany). The cutting parameters were set at a rotational speed of 3000 RPM and a feed rate of 0.25 mm/s, utilizing a diamond-tipped cutting disc of B0D15 grade.

Two notches were added to the dog-bone specimen to localize stresses and define a region of interest for Digital Image Correlation (DIC) analysis. In situ mechanical testing was conducted using a Deben Microtest 1 kN tensile stage (Deben Ltd., UK) in combination with an Altami 6C optical microscope (Altami, Russia). The tensile test was performed at a constant crosshead speed of 0.5 mm/min. Images were captured by the optical microscope at a rate five times faster than the testing speed, with a resolution of 1024×768 pixels. The post-processing DIC analysis of the acquired images was done using Matlab-based open-source software [20].

The rectangular bar was used for microstructural analysis. It was sequentially ground using silicon carbide sandpaper with grit sizes of 320, 500, 800, 1000, and 2000 to achieve a smooth, plane-parallel surface. This was followed by polishing with coarse polishing cloths (MD-Mol and MD-Pan) using diamond suspensions (DiaDuo-2) with grain sizes of 6, 3, and 1 μm. For the final polishing step, a fine MD-Chem cloth was used with colloidal silica suspension (OPS). Grinding and polishing were performed using LaboSystem equipment (LaboSystem, Belgium) with consumables from Struers. The final stage of sample preparation involved rinsing with distilled water and vacuum drying at 40°C for 2 hours.

RESULTS AND DISCUSSION

Prior to conducting the in situ mechanical testing of the samples, the structure and morphology of the cross-sectional area of the CFRP were carefully examined using scanning electron microscopy. The results of this microstructural characterization are presented in Fig. 1. Each sub-image (a-e) highlights distinct features pertinent to the analysis of fiber alignment, packing, defects, and interfacial regions within the composite.

Fig. 1(a) shows a low-magnification view capturing two layers of the composite structure with different fiber orientations: 90° on the left and 0° on the right. This image provides insights into key structural characteristics of the composite. The average diameter of the carbon fibers ranges from 5 to 7 μm, while the average thickness of each layer is approximately 200 μm. A gap of around 30 μm is observed between every five layers, as further illustrated in Fig. 1(d). Additionally, a small void was observed within the layer of longitudinally aligned fibers, close to the interface with the layer of perpendicularly oriented fibers; this void is marked with a red circle.

A closer examination of the cross-sectional area is provided in Figs. 1(b), 1(c), and 1(e). Labels 1 and 2 identify distinct regions within the composite. Region 1 corresponds to a high-quality epoxy matrix surrounding the fibers, highlighting regular fiber packing and circular cross-sections. In contrast, region 2 reveals areas with flaws in the epoxy matrix, indicating lower matrix quality and visible defects. Furthermore, red and yellow arrows mark possible interfacial gaps and micro- or nano-scale voids. These voids or gaps could serve as stress concentrators, potentially affecting the mechanical properties of the composite.

Fig. 1(d) shows the "brook" between the two layers. This feature, attributed to the specific manufacturing technique used, is designed to ensure uniform impregnation of the fibers by the matrix material. Such structural considerations are critical for achieving optimal mechanical performance by promoting effective bonding and load transfer between the fibers and matrix.

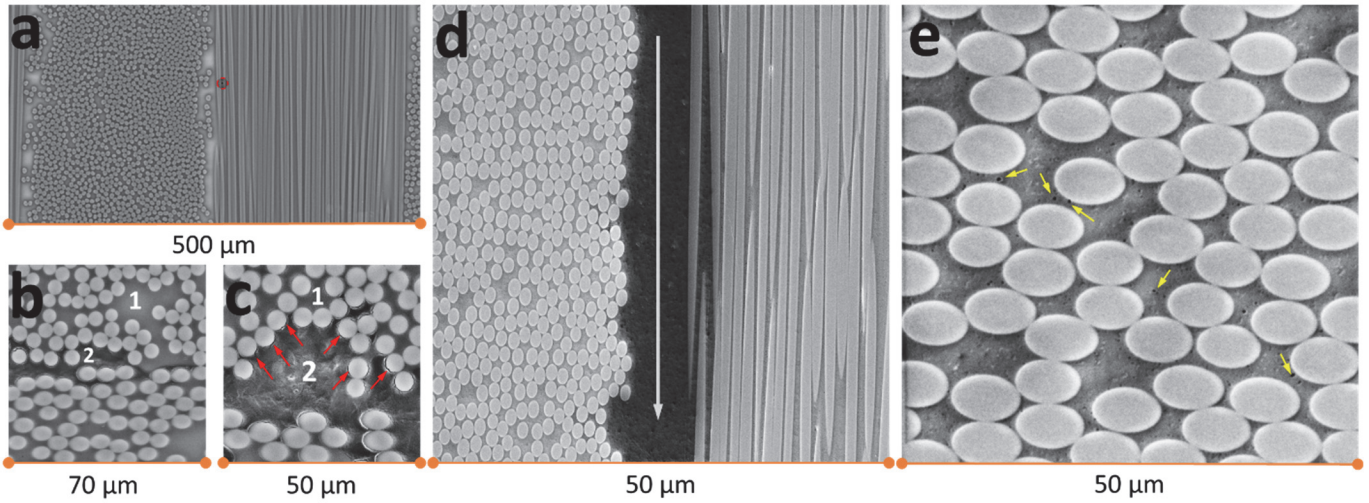

Figure 1: Micrographs of the cross-sectional morphology of the CFRP composite structure. (a) Low-magnification view showing two distinct layers with fiber orientations of 90° (left) and 0° (right). A small void near the interface between these layers is marked with a red circle. (b,c) Higher magnification images of the cross-section, with labels 1 and 2 identifying regions of high-quality and flawed epoxy matrix, respectively. Red arrows indicate potential interfacial gaps and microvoids. (d) "Brook" feature between layers, designed to ensure uniform fiber impregnation during manufacturing. (e) High-magnification view showing nanoscale pores in the epoxy matrix, indicated by yellow arrows.

The force-displacement curve obtained during in situ tensile testing of the CFRP dog-bone-shaped composite sample is presented in Fig. 2(a). Several stages can be identified in this curve, each corresponding to distinct processes occurring during the test. The initial segment of the curve, up to the dashed gray vertical line, represents the movement of the specimen within the grips, which typically involves adjusting to eliminate slack and establish contact with the sample. Following this, a small drop in force is observed at the intersection with the dashed green line, indicating the onset of local damage within the material. This local damage does not compromise the overall structural integrity of the composite; however, it signifies the beginning of minor matrix or fiber-matrix debonding, which could act as a precursor to further damage under continued loading.

Fig. 2(b) illustrates the average strain evolution in the *xx*, *xy*, and *yy* directions. These strain components were calculated by averaging 2D strain maps derived from DIC analysis throughout the experiment. Notably, the strain components ε_{xx} and ε_{xy} exhibit a peak at frame number 18, with a strain magnitude of approximately 0.015 (1.5 %). This frame, marked as a red point on the force-displacement curve, signifies a critical point in the test. Beyond this point, the composite begins to experience a significant reduction in structural integrity due to the accumulation of intense shear and normal strains along the x direction. These strains promote debonding between composite layers and even partial delamination or layer disappearance, as observed in Fig. 3(a).

The strain curves also highlight that shear strain, particularly ε_{xy}, is the primary mechanism affecting the mechanical stability of the composite. This component shows a steady increase from the beginning of the test, intensifying up to the critical point, which suggests that shear forces contribute most significantly to the progressive degradation of the material. Figs. 2(c-e) display the strain distributions for ε_{xx}, ε_{xy}, and ε_{yy} at the critical state marked by the red point on the force-displacement curve. These strain maps reveal localized areas of high strain concentration, especially in the shear component, further supporting the role of shear-induced damage in the composite's failure process.

Despite the onset of significant damage, the composite retains a residual load-bearing capacity even after reaching the critical point, as indicated by the continued rise in the force-displacement curve. This observation suggests that, while the composite's structural integrity is compromised, it can still withstand additional loading to some extent, highlighting a degree of damage tolerance inherent in the material design.

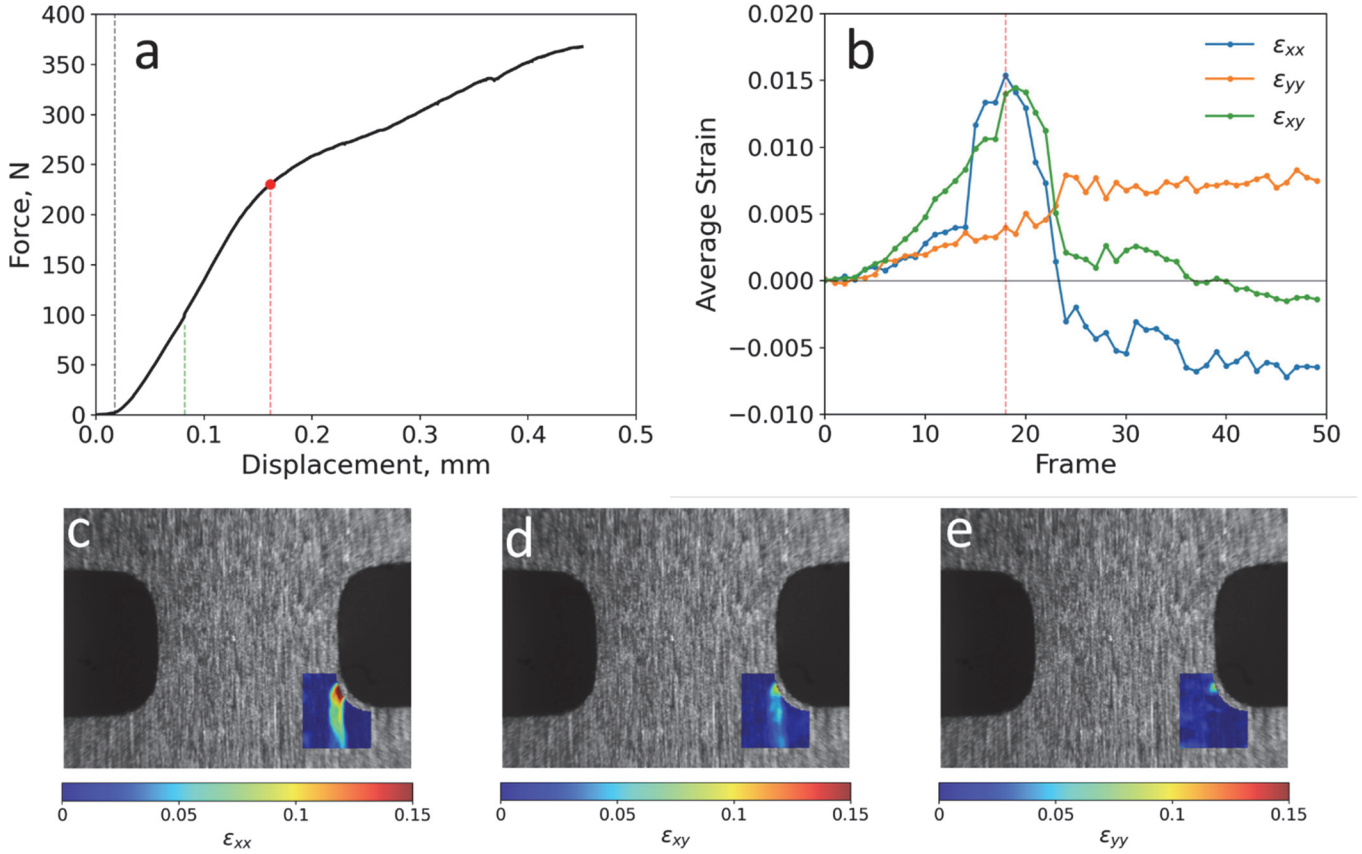

Figure 2: Mechanical analysis of the CFRP dog-bone sample under in situ tensile testing. (a) Force-displacement curve illustrating multiple stages of the tensile test. The initial segment up to the dashed gray line represents specimen adjustment within the grips. A small drop in force at the green dashed line indicates the onset of localized damage within the composite. The red point marks the critical moment, where peaks of shear and normal strains in the x direction are observed, signifying the start of significant structural degradation. (b) Evolution of average strain components ε_{xx}, ε_{xy}, and ε_{yy} over time (direct correlation with frames captured during experiment), calculated from DIC-based 2D strain maps. (c-e) Strain distribution maps for ε_{xx}, ε_{xy}, and ε_{yy} at the critical point, showing localized areas of high strain concentration, which contributes to progressive damage within the composite.

The microstructure characterization after in situ tension of the dog-bone-shaped specimen is depicted in Fig. 3. A general macroscale view of the specimen cross-section is illustrated in Fig. 3(a). It is observed that several layers of the composite

were completely destroyed and partially removed from the specimen. A high-magnification SEM image of the sample, focusing on the surface and edge details of the notches, is shown in Fig. 3(b). The two enlarged insets on the left and right, outlined by dashed yellow boxes, highlight regions with highest strain concentrations of the sample.

The sample revealed prominent damage along the central region, where fibers and matrix material have separated, indicating delamination and matrix cracking as a result of mechanical stress. Key features observed include:

- Delamination: The vertical splitting along the fiber direction suggests debonding between layers, a common failure mode in fiber-reinforced composites under tensile loading. This separation indicates a loss of cohesion between the fiber and matrix, likely due to shear stresses and fiber pull-out during testing.
- Matrix Cracking: Fine, irregular cracks are visible within the matrix material, especially around the central region of the fracture. These cracks are indicative of the brittle nature of the epoxy matrix, which can lead to rapid failure once the matrix is overstressed.
- Fiber Pull-out and Shear Failure: In certain regions, fibers appear to have been pulled out or misaligned, which suggests fiber-matrix interface failure and shear forces at play. These features highlight areas where the composite has experienced concentrated stress, leading to localized fiber breakage or slippage.

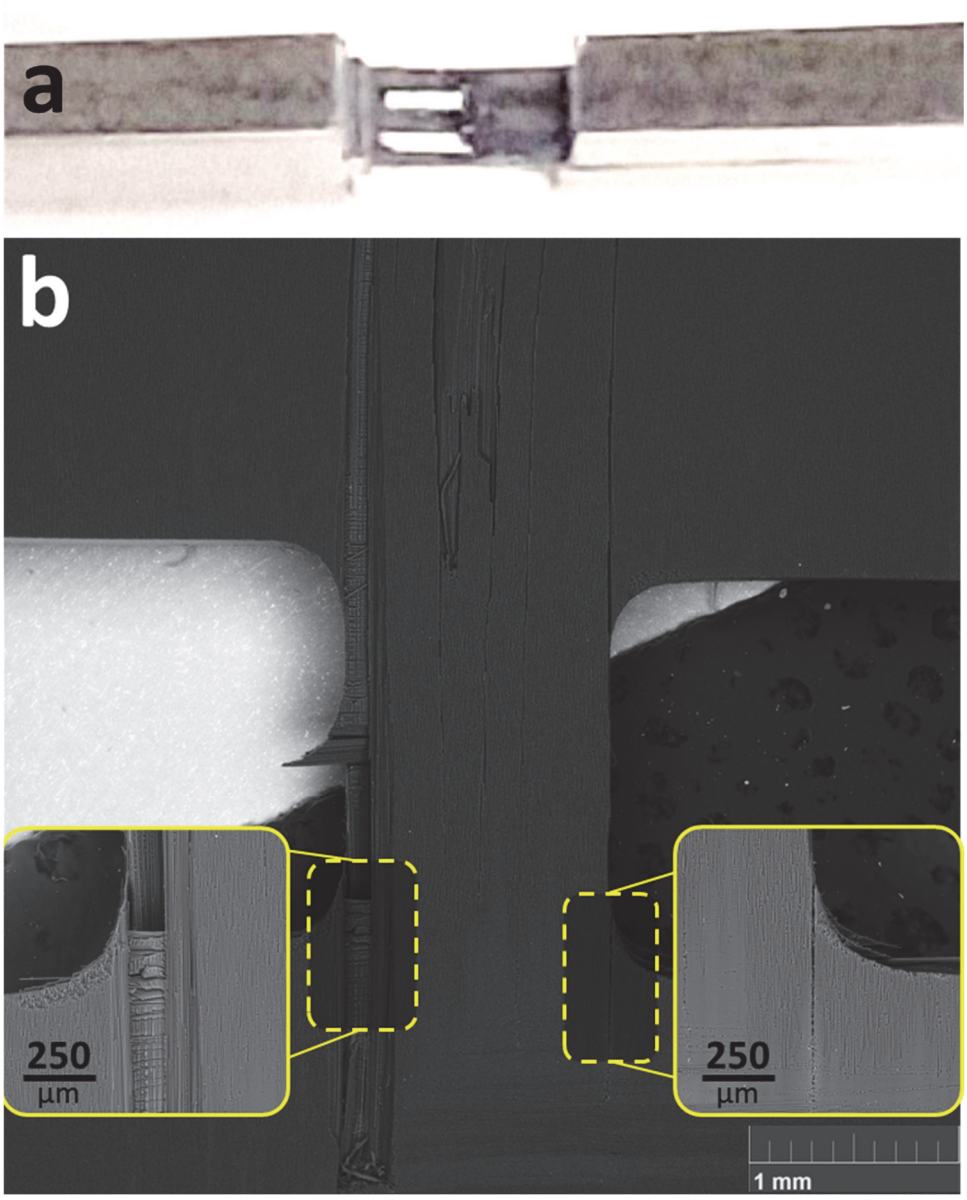

Figure 3: The structure characterization of the dog-bone-shaped specimen after in situ tension: (a) macroscale view of the specimen cross-section; (b) fracture locations.

Conclusions

The in situ tensile testing of the CFRP composite sample, along with detailed microstructural analysis, provided important insights into how this material behaves under mechanical stress. Initial imaging of the composite structure revealed key aspects of fiber alignment, density, and bonding with the epoxy matrix, as well as minor defects that could act as stress points and influence the material's performance.

During testing, different stages of stress response at the force-displacement curve were identified. Early in the process, a minor force drop suggested the onset of localized damage within the composite, likely involving small-scale cracking or separation between the fibers and matrix. While this initial damage did not compromise the material's overall structure, it marked the start of weakening at the interface between the matrix and fibers.

Further analysis highlighted an increase in shear and normal strains in x direction, which both reached a peak at a critical point during the test. This strain build-up led to progressive damage, such as layer separation and internal cracking, driven largely by shear forces. Observations after the test showed clear signs of delamination, matrix cracking, and fiber pull-out, all of which are typical failure modes in fiber-reinforced composites under load.

Despite the damage, the composite was able to bear additional load beyond the critical point, showing some degree of resilience. Overall, this study illustrates the complexity of failure mechanisms in CFRP materials, highlighting the role of shear forces and interface integrity in their structural performance. These findings provide a foundation for improving CFRP composites in applications that demand strength and durability, offering insights for optimizing material design and manufacturing.

In future work, modeling will extend insights gained from in situ tensile testing of CFRP composites, focusing on damage progression at the fiber-matrix interface and within the matrix itself. The model will use a cohesive zone approach to simulate initial interfacial damage and finite element analysis (FEA) to track shear and normal strain peaks in the x-direction, which drive progressive failures like delamination, matrix cracking, and fiber pull-out. Additionally, the model will assess the composite's post-critical load-bearing capacity, replicating its resilience despite progressive damage. This integrated approach will validate experimental force-displacement curves, offering valuable guidance for optimizing CFRP design for enhanced durability.

Acknowledgements

This study was carried out under the Agreement for the provision of grant funding from the federal budget for large scientific projects in priority areas of scientific and technological development of the Russian Ministry of Science and Higher Education no. 075-15-2024-552.

References

[1] Soutis, C. (2005). Carbon fiber reinforced plastics in aircraft construction, Materials Science and Engineering A, 412(1–2), pp. 171–176. DOI: 10.1016/j.msea.2005.08.064.

[2] Bellonte, M. (2001). Composite materials in the Airbus A380 - From history to future.

[3] Ahmad, F., Awadh, M.A., Abas, M., Noor, S., Hameed, A. (2022). Optimization of carbon fiber reinforced plastic curing parameters for aerospace application, Applied Sciences, 12(9), p. 4307. DOI: 10.3390/app12094307.

[4] Ahmad, H., Markina, A.A., Porotnikov, M.V., Ahmad, F. (2020). A review of carbon fiber materials in automotive industry, IOP Conference Series Materials Science and Engineering, 971(3), p. 032011. DOI: 10.1088/1757-899x/971/3/032011.

[5] Automobiles - Carbon Fiber & Carbon Fiber Reinforced Plastics Case study - Mitsubishi Chemical Carbon Fiber & Carbon Fiber Reinforced Plastics Special Site. (n.d.). Available at: https://www.m-chemical.co.jp/carbon-fiber/en/case/car/.

[6] Sreejith, M., Rajeev, R.S. (2021). Fiber reinforced composites for aerospace and sports applications., Elsevier eBooks, pp. 821–859.

[7] Zhang, J.Z. (2013). Study on Carbon fiber composite materials in sports equipment, Applied Mechanics and Materials, 329, pp. 105–108. DOI: 10.4028/www.scientific.net/amm.329.105.

[8] Towsyfyan, H., Biguri, A., Boardman, R., Blumensath, T. (2019). Successes and challenges in non-destructive testing of aircraft composite structures, Chinese Journal of Aeronautics, 33(3), pp. 771–791. DOI: 10.1016/j.cja.2019.09.017.

[9] Mechanical testing of composites. (n.d.).
Available at: https://www.addcomposites.com/post/mechanical-testing-of-composites.
[10] Kennedy, S.M., Robert, R.J., Prince, R.M.R., Hikku, G., Kaliraj, M. (2024). A Comprehensive overview of the Fabrication and Testing Methods of FRP Composite Pipes, MethodsX, p. 102990. DOI: 10.1016/j.mex.2024.102990.
[11] Andrew, J.J., Srinivasan, S.M., Arockiarajan, A., Dhakal, H.N. (2019). Parameters influencing the impact response of fiber-reinforced polymer matrix composite materials: A critical review, Composite Structures, 224, p. 111007.
DOI: 10.1016/j.compstruct.2019.111007.
[12] Karataş, M.A., Gökkaya, H. (2018). A review on machinability of carbon fiber reinforced polymer (CFRP) and glass fiber reinforced polymer (GFRP) composite materials, Defence Technology, 14(4), pp. 318–326.
DOI: 10.1016/j.dt.2018.02.001.
[13] Ghaffari, S., Seon, G., Makeev, A. (2020). In-situ SEM based method for assessing fiber-matrix interface shear strength in CFRPs, Materials & Design, 197, p. 109242. DOI: 10.1016/j.matdes.2020.109242.
[14] Zhang, B., Ge, J., Cheng, F., Huang, J., Liu, S., Liang, J. (2023). Failure prediction for fiber reinforced polymer composites based on virtual experimental tests, Journal of Materials Research and Technology, 24, pp. 8924–8939.
DOI: 10.1016/j.jmrt.2023.05.123.
[15] Statnik, E.S., Nyaza, K.V., Salimon, A.I., Ryabov, D., Korsunsky, A.M. (2021). In situ SEM study of the Micro-Mechanical Behaviour of 3D-Printed Aluminium Alloy, Technologies, 9(1), p. 21. DOI: 10.3390/technologies9010021.
[16] Statnik, E.S., Cvjetinovic, J., Ignatyev, S.D., Wassouf, L., Salimon, A.I., Korsunsky, A.M. (2023). Hair-Reinforced Elastomer Matrix Composites: formulation, mechanical testing, and advanced microstructural characterization, Polymers, 15(22), p. 4448. DOI: 10.3390/polym15224448.
[17] Hapke, J., Gehrig, F., Huber, N., Schulte, K., Lilleodden, E.T. (2011). Compressive failure of UD-CFRP containing void defects: In situ SEM microanalysis, Composites Science and Technology, 71(9), pp. 1242–1249.
DOI: 10.1016/j.compscitech.2011.04.009.
[18] Rudolf, C., Boesl, B., Agarwal, A. (2015). In situ Mechanical Testing Techniques for Real-Time Materials Deformation Characterization, JOM, 68(1), pp. 136–142. DOI: 10.1007/s11837-015-1629-8.
[19] Morokov, E., Titov, S., Levin, V. (2022). In situ high-resolution ultrasonic visualization of damage evolution in the volume of quasi-isotropic CFRP laminates under tension, Composites Part B Engineering, 247, p. 110360.
DOI: 10.1016/j.compositesb.2022.110360.
[20] Ncorr - Open source 2D digital image correlation MATLAB software. (n.d.). Available at: http://www.ncorr.com/.